



## **Fast in-situ annealing stage coupled with EBSD: A suitable tool to observe quick recrystallization mechanisms**

Nathalie Bozzolo, Suzanne Jacomet, Roland E. Logé

### **► To cite this version:**

Nathalie Bozzolo, Suzanne Jacomet, Roland E. Logé. Fast in-situ annealing stage coupled with EBSD: A suitable tool to observe quick recrystallization mechanisms. *Materials Characterization*, 2012, 70, pp.28-32. <10.1016/j.matchar.2012.04.020>. <hal-00709665>

**HAL Id: hal-00709665**

**<https://minesparis-psl.hal.science/hal-00709665v1>**

Submitted on 22 Aug 2012

**HAL** is a multi-disciplinary open access archive for the deposit and dissemination of scientific research documents, whether they are published or not. The documents may come from teaching and research institutions in France or abroad, or from public or private research centers.

L'archive ouverte pluridisciplinaire **HAL**, est destinée au dépôt et à la diffusion de documents scientifiques de niveau recherche, publiés ou non, émanant des établissements d'enseignement et de recherche français ou étrangers, des laboratoires publics ou privés.



HAL Authorization

# **Fast in-situ annealing stage coupled with EBSD : a suitable tool to observe quick recrystallization mechanisms**

N. Bozzolo<sup>\*</sup>, S. Jacomet, and R.E. Logé

Mines ParisTech, CEMEF - Center of Materials Forming

CNRS UMR 7635, BP 207

F-06904 Sophia Antipolis Cedex, France

<sup>\*</sup> corresponding author :

e-mail : [nathalie.bozzolo@mines-paristech.fr](mailto:nathalie.bozzolo@mines-paristech.fr)

phone number : +33(0) 493 6789 45

**Abstract.** A heating stage as been developed to perform in-situ annealing in a SEM equipped with an EBSD system in order to study recrystallization mechanisms. High temperature treatments could then be performed inside the SEM, up to 1180°C and with high heating- and cooling-rates ( $\sim 100^{\circ}\text{C.s}^{-1}$ ). Samples were cooled down to room temperature to perform EBSD orientation mapping in between successive short-duration heat-treatments. Microstructure evolution snapshots obtained this way allow gaining an insight into recrystallization mechanisms. The interest of such experiments is shown for two examples: static recrystallization of cold-deformed pure tantalum, and post dynamic evolution of hot-deformed Zircaloy4.

**Keywords:** EBSD, in-situ annealing, recrystallization, tantalum, zirconium

## **1. Introduction**

Understanding recrystallization in polycrystalline materials, as well as any microstructure evolution phenomenon, requires a description of the physical mechanisms which occur locally and to observe how these mechanisms depend on microstructure local parameters. One of the main difficulties to overcome is linked to the fact that once the phenomenon occurred (e.g. a nucleus appeared, or a grain boundary moved), the pre-existing structures have disappeared. Identifying recrystallization mechanisms from a series of samples annealed under different conditions must therefore be based on statistical considerations. An alternative approach is to observe how a particular local structure evolves during annealing and check if this evolution is consistent with the postulated physical mechanism. The possibility of directly observing the evolution of a given sample area in the deformed state and throughout recrystallization is then of utmost interest. The use of an in-situ heating stage in a SEM system offers that possibility [1,2]. SEM provides the suitable spatial resolution, and, if coupled to the EBSD technique, also allows for investigating

local texture effects which are of utmost importance when dealing with grain boundary migration phenomena.

Studying recrystallization mechanisms (notably the nucleation stage) has motivated the development of in-situ annealing devices over the last decade. The main drawbacks of the previously developed devices were a relatively low maximal temperature (typically 500°C) or a rather slow heating rate (only few °C.s<sup>-1</sup>) [3-6], and a poor control of temperature gradients within the sample. More recently, high-temperature in-situ annealing treatments (>1000°C) have been performed by D. Prior's team in Liverpool, with a heating stage implemented in a CAMSCAN SEM especially designed for in-situ experiments [7,8]. In addition, in those experiments, controlling the heating and cooling rates is not that crucial because EBSD data are directly acquired at high temperature. The increase in EBSD data acquisition rates indeed allows nowadays for getting the zone of interest scanned within a few minutes, which can be achieved if the required spatial resolution is not too high or the scanned area not too large. Such an experimental procedure is nevertheless suitable only if the evolution kinetics are slow enough [9,10]. In order to avoid those limitations, we adopted the sequential approach which consists in room temperature EBSD measurements after successive annealing treatments. Then heating and cooling must be as fast as possible so that the microstructure does not evolve during heating and cooling stages. The observed evolution can then be related to the holding time at the chosen annealing temperature. It is worth noticing that if this sequential approach has advantages for recrystallization and grain growth studies, it would not be suitable for other processes like phase transformations. In this case, EBSD mapping at high temperature is required [11].

The main design differences between the previously existing heating stages lies on the sample dimensions and how it is connected to the heating device. Systems with a relatively massive sample, including commercial ones, have a thermal inertia which does not allow for fast heating and cooling. In addition, thermal gradients may still exist in the sample and the temperature reached at the observed surface may be difficult to determine [12]. This is one of the main reasons why we, and other teams [e.g. 13], have chosen to build a heating stage based on the principle originally proposed by R. Le Gall et al. [3]. This principle and how it was adapted is described in the next section. In the following, recrystallization sequences obtained by this technique will be presented and discussed.

## 2. Experimental setup

An in-situ heating stage has been developed to be set up in a FEI XL30 ESEM also equipped with a TSL EBSD system (view of the heating stage tilted to 70° in the SEM chamber, as required for EBSD measurements, in Fig. 1a). The basic principle of this heating stage has originally been

proposed by R. Le Gall et al. [3]. The heating device is a thin tantalum foil (about 30  $\mu\text{m}$  thick) on which the sample (few mm wide and  $\sim 300\ \mu\text{m}$  thick) is point-welded (Fig. 1b). An electrical current goes through the Ta foil such that both the Ta foil and the sample are heated by Joule effect. Thanks to the small dimensions, a power of only a few tens of Watts is sufficient to achieve high temperature (1200°C has easily been reached), and temperature is very likely to be homogeneous in such thin pieces. Another advantage is the low thermal inertia which allows fast heating and cooling (both at  $\sim 100^\circ\text{C.s}^{-1}$ ). Our original contribution to this design mainly lies in the Ta plate being mounted on a mechanical system that compensate for thermal dilatation. This allows for keeping the zone of interest in the same position throughout the heating-annealing-and-cooling cycles. In addition, in our system, the temperature cycles are program-controlled using thermocouples welded on the sample surface (Fig. 1b).

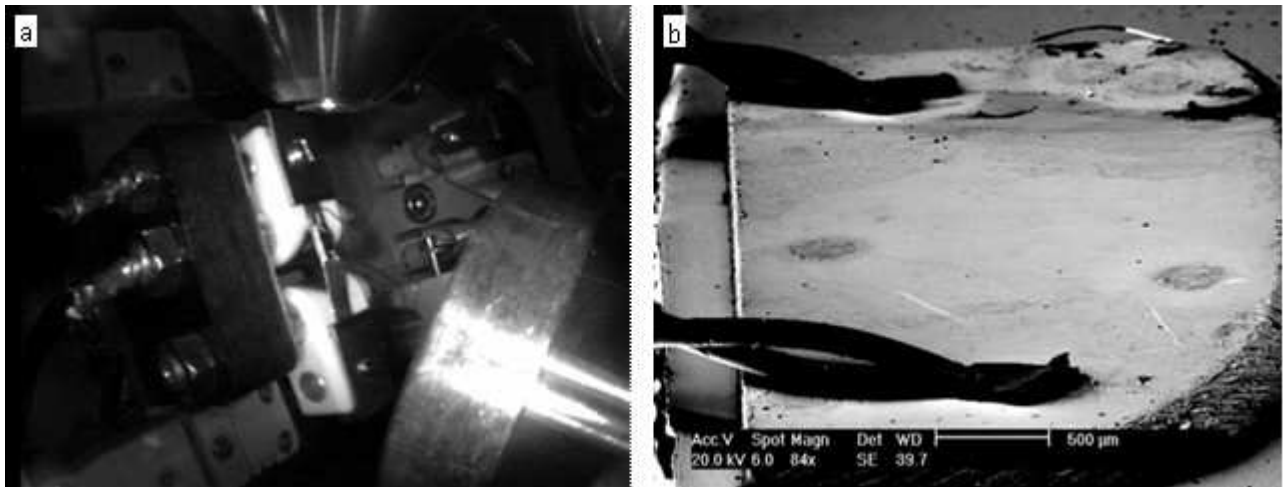


Figure 1. a) Heating stage mounted in the SEM chamber, tilted to 70° to suit EBSD settings. b) Thermocouples welded on the sample which itself is welded on the Ta plate.

### 3. Recrystallization sequences

#### 3.1. Static recrystallization of tantalum (more details in [14]).

Pure tantalum, which was initially in fully recrystallized state with equiaxed grains, was deformed by compression at room temperature. This led to a heterogeneously deformed microstructure (Fig. 2a). All the grains flattened but some of them accumulated more internal strain than others as revealed by higher Kernel Average Misorientation (KAM) values.

During the first annealing steps, the intragranular misorientations decrease in amplitude as a result of recovery, the peak in the KAM distribution shifts to lower values. Then, recrystallized grains appear (top of microstructure 3d) in the areas which initially had high KAM values. Subsequently, the recrystallized grains progressively invade the recovered matrix. They are characterized by low KAM values and, accordingly, a distinct peak centered on  $0.5^\circ$  appears and increases in the KAM distribution. The last unrecrystallized grains in microstructure 3f correspond to those with low KAM in the deformed state. Such a behavior has already been reported for tantalum, with much coarser grains [15-17]. Assuming that the KAM value is increasing with increasing strain and therefore with increasing stored energy, the dependence of the local recrystallization kinetics with the stored energy level could be directly observed in those experiments.

The large recrystallized grains (Figs. 3e-f) exhibit island grains, with high KAM values, through which the moving boundary could not go. Further experiments have to be done to check whether this is an intrinsic behavior of the material or if this is an artifact resulting from the free surface effects. In addition, the indexing rate is much lower after the first heating steps than it is in the deformed state, which sounds counterintuitive. The indexing rate is subsequently improved while recrystallization progresses. If oxidation was responsible for the lower indexing rate after heating, it would not vanish later on. One possible explanation, which will also require further investigations, is that dislocations may be attracted near the surface and affect the diffraction diagram quality. It is worth noticing that the material of this experiment was a high purity metal, in which the mobilities of both dislocations and grains boundaries are known to be higher than in alloys. Such a material is more likely to be sensitive to free surface effects.



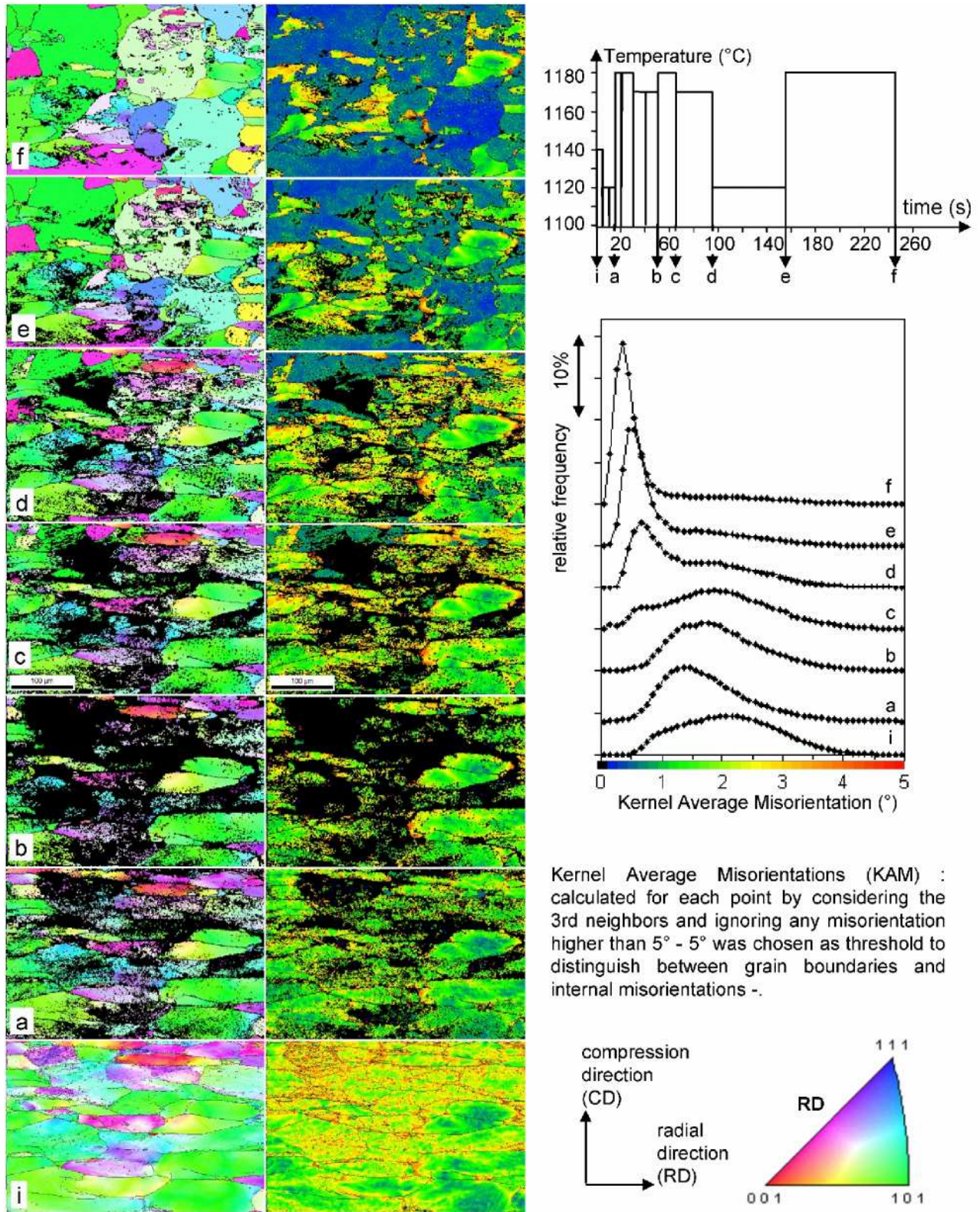


**Figure 2.** Recrystallization sequence of cold deformed tantalum: i) and a-f) Microstructure as revealed by EBSD for the initial state and after successive heat treatments detailed in the top right graph. For each state, the microstructure is shown within a orientation color-coded (left column; radial direction RD projected in the standard triangle) and within a color code defined as function of the KAM value (right column; blue to red for KAM = 0 to 5°). A kernel radius of 3μm was considered for KAM calculations. The evolution of the KAM angle distribution is also shown on the right part of the figure. Black pixels are non-indexed points. EBSD scan step size: 1μm

### 3.2. Post-dynamic recrystallization of Zircaloy-4 (more details in [18]).

A sample was taken from the core of a hot-extruded bar of Zircaloy4, which was initially in a  $\beta$ -quenched state. The extrusion conditions were chosen to avoid post-dynamic recrystallization because the aim of these experiments was precisely to provide information about the post-dynamic microstructure evolution. The initial hot-extruded specimens (Fig. 3a) therefore exhibit a duplex microstructure made of (i) highly-recovered / continuously-recrystallized small equiaxed grains, and (ii) elongated strain-hardened grains. The non-fragmented lamellar structures exhibit orientation spread and accordingly color gradients. Both continuous orientation gradients and substructures are visible. Apart from those lamellar areas, EBSD patterns could seldom be reliably indexed, because of the small size of dynamically-recrystallized-grains and recovered grain-fragments, which were below the actual spatial resolution of EBSD mapping in the used SEM.

Upon heat treatment (Figs. 3b-c), fast recrystallization is observed in the fragmented part, fast growth of existing equiaxed small grains is observed and also new grains seem to appear from areas where the orientation could not be measured in the initial material. These "new" grains are in fact very likely to arise from the growth of small dynamically-recrystallized grains or recovered fragments. This stage is achieved within the first 15 sec at 750°C. Such a fast evolution can not be assessed by conventional bulk specimen annealing, because controlling a holding time of a few seconds at a high target temperature reached at high heating speed is almost impossible.

The fast early stage is followed by a slower evolution of the elongated grain structures. The internal structure of the initial lamellae reorganizes by recovery but most of these lamellae still remain after the three successive annealing treatments of 5s at 750°C. Orientations with  $\langle 10\text{-}10 \rangle$  close to the extrusion direction are predominant in the initial material and orientations with  $\langle 11\text{-}20 \rangle$  develop during recrystallization, especially for the largest recrystallized grains. Both the two-stage recrystallization kinetics and the crystallographic texture change are fully consistent with the results reported for conventional studies of static recrystallization in cold deformed low alloyed zirconium [19-21]. This suggests that the interaction of the free surface with the crystalline defects and the moving grain boundaries did not change much the recrystallization mechanisms in those in-situ experiments as compared to what happens in the bulk.

In the cited static recrystallization studies, annealing was performed at lower temperature to slow down kinetics and observe the early evolution stages. In the present experiment, the temperature was chosen to match the industrial forming temperature of the Zircaloy-4, in-situ annealing was the only way to observe the very fast early stages of post-dynamic recrystallization.



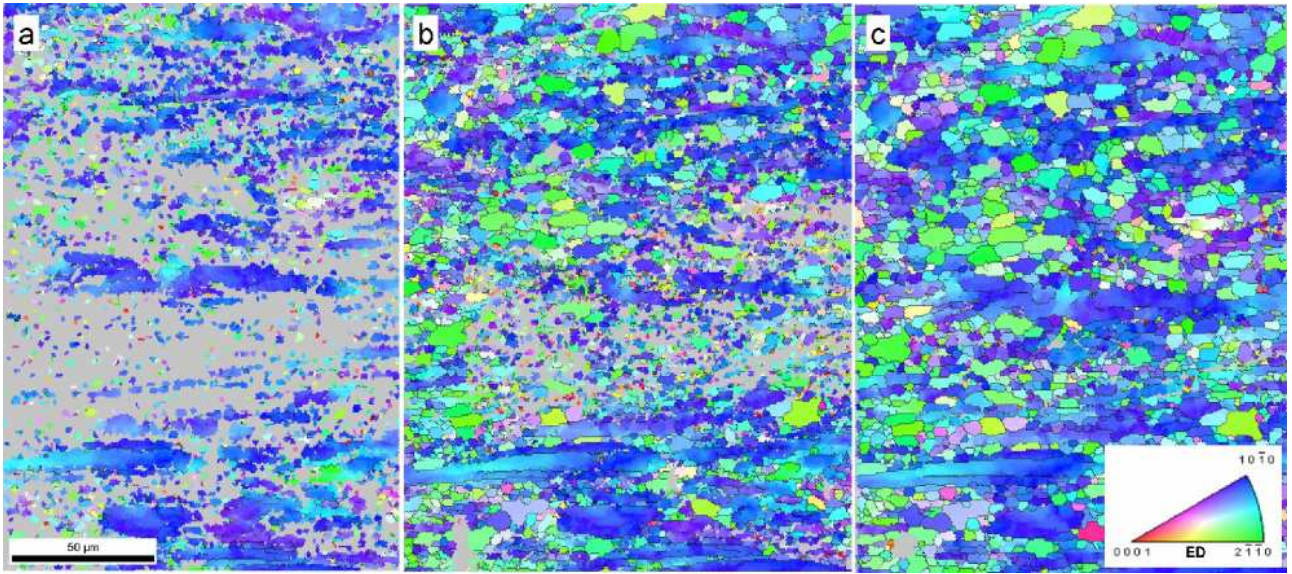


**Figure 3.** Recrystallization sequence of a Zy4 sample. a) initial state (hot-extruded at 685°C and cooled down rapidly). Microstructure after b) two, c) three, successive 5s in-situ annealing treatments at 750°C. Extrusion direction is horizontal, radial direction vertical, the color code defined on the inverse pole figure refers to the extrusion direction. The grey pixels are those for which the orientation could not be reliably determined. EBSD scan step size: 0.75μm.

#### 4. Conclusion and prospects

The approach involving in-situ annealing and observation of recrystallization phenomena at a free surface was criticized in the past with the argument that phenomena at the sample surface may differ from those in the bulk. The observed free surface indeed interacts with crystalline defects and moving boundaries. This may nevertheless be more harmful for i) pure metals (e.g. pure tantalum data shown here) and ii) for curvature-driven grain boundary motion than for recrystallization phenomena (which involve much higher driving forces).

Providing a careful interpretation, our in-situ annealing device coupled with EBSD characterization can provide information about the recrystallization mechanisms which can not be assessed otherwise. A typical example was shown here for post-dynamic recrystallization at 750°C in the zirconium alloy, where the fast early evolution achieved within 15 seconds could be sequentially observed. This technique will be improved, notably by coupling it with a FEG-SEM and a fast EBSD camera to improve the spatial resolution of the EBSD maps, so that the phenomena can not only be observed, but the related fine-scale mechanisms can be identified. The output of these in-situ annealing experiments will also be deeper analyzed i) by detecting more precisely where changes occur (this can be done for example by calculating the orientation change for each point in the map between two successive snapshots, i.e. calculating "time-lapse misorientation maps" as proposed recently by Wheeler et al. [22]), and ii) by evaluating semi-quantitatively the stored energy field (via the local content of geometrically necessary dislocations assessed from the intragranular misorientations [23-26]).



## Acknowledgements.

The authors are very grateful to the CEMEF-MEA staff that has designed and made the heating-stage, and to Marie Houillon and Benoit Gaudout for providing the two examples shown here.

## References

- [1] F.J. Humphreys, M. Ferry, C.P. Johnson, I. Brough "Combined in situ annealing and EBSD of deformed alloys" *Textures and Microstructures* 26-27 (1996) 281
- [2] S.I. Wright, and M. Nowell "A review of in situ EBSD studies" in *Electron Backscatter Diffraction in Materials Science*, A.J. Schwartz et al. (eds.), © Springer Science + Business Media, LCC 2009
- [3] G.J. Liao, R. Le Gall, G. Saindrenan "Experimental investigations into kinetics of recrystallisation of cold rolled nickel": *Materials Science and Technology* 14 (1998), 411
- [4] Y. Huang, F.J. Humphreys "Measurements of grain boundary mobility during recrystallization of a single-phase aluminium alloy": *Acta Materialia* 47:7 (1999) 2259
- [5] M. Kiaei, R. Chiron, B. Bacroix "Investigation of recrystallization mechanisms in steels during in situ annealing in a sem" *Scripta Materialia* 36:6 (1997) 659
- [6] P.J. Hurley, F.J. Humphreys "A study of recrystallization in single-phase aluminium using in-situ annealing in the scanning electron microscope" *Journal of Microscopy-Oxford* 213 (2004) 225
- [7] C.G.E. Seward, D.J. Prior, J. Wheeler, S. Celotto, D.J.M. Halliday, R.S. Paden, M.R. Tye "High-temperature electron backscatter diffraction and scanning electron microscopy imaging techniques: In-situ investigations of dynamic processes" *Scanning* 24:5 (2002) 232
- [8] C.G.E. Seward, S. Celotto, D.J. Prior, J. Wheeler, R.C. Pond "In situ SEM-EBSD observations of the hcp to bcc phase transformation in commercially pure titanium" *Acta Materialia* 52 (2004) 821
- [9] K. Mirpuri, H. Wendrock, S. Menzel, K. Wetzig, J. Szpunar "Texture evolution in Copper film at high temperature studied in situ by electron back-scatter diffraction" *Thin Solid Films* 496 (2006) 703
- [10] D.P. Field, L.T. Bradford, M.M. Nowell, T.M. Lillo "The role of annealing twins during recrystallization of Cu" *Acta Materialia* 55 (2007) 4233
- [11] C.G.E. Seward, S. Celotto, D.J. Prior, J. Wheeler, R.C. Pond "In situ SEM-EBSD observations of the hcp to bcc phase transformation in commercially pure titanium" *Acta Materialia* 52 (2004) 821
- [12] M. Bestmann, S. Piazzolo, C.J. Spiers, D.J. Prior "Microstructural evolution during initial stages of static recovery and recrystallization: new insights from in-situ heating experiments combined with electron backscatter diffraction analysis" *Journal of Structural Geology* 27 (2005) 447

- [13] A. Lens, C. Maurice, J.H. Driver "Grain boundary mobilities during recrystallization of Al-Mn alloys as measured by in situ annealing experiments " *Materials Science and Engineering A* 403 (2005) 144
- [14] M. Houillon "Numerical modelling of flow forming on tantalum and subsequent heat treatment" PhD thesis, Mines-Paristech (2009)
- [15] H. R.Z. Sandim, A. F. Padilha, V. Randle, W. Blum "Grain subdivision and recrystallization in oligocrystalline tantalum during cold swaging and subsequent annealing" *International Journal of Refractory Metals & Hard Materials* 17 (1999) 431
- [16] H. R. Z. Sandim, J. P. Martins and A. F. Padilha "Orientation effects during grain subdivision and subsequent annealing in coarse-grained tantalum" *Scripta Materialia* 45:6 (2001) 733
- [17] H.R.Z. Sandim, J.P. Martins, A.L. Pinto, A.F. Padilha "Recrystallization of oligocrystalline tantalum deformed by cold rolling" *Materials Science and Engineering A* 392 (2005) 209
- [18] B. Gaudout "Microstructural modelling and lubrication study during zirconium alloy hot extrusion" PhD thesis, Mines-Paristech (2009)
- [19] N. Dewobroto, N. Bozzolo, P.Barberis and F. Wagner "Experimental investigations of recrystallization texture development in zirconium (Zr702)" *Materials Science Forum* 467-470 (2004) 453
- [20] K.Y. Zhu, D. Chaubet, B. Bacroix, F. Brisset "A study of recovery and primary recrystallization mechanisms in a Zr-2Hf alloy" *Acta Materialia* 53 (2005) 5131
- [21] N. Dewobroto, N. Bozzolo, P.Barberis and F. Wagner "On the mechanisms governing the texture and microstructure evolution during static recrystallization and grain growth of low alloyed zirconium sheets (Zr702)" *International Journal of Materials Research* 97 (2006) 6
- [22] J. Wheeler, A. Cross, M. Drury, R.M. Hough, E. Mariani, S. Piazzolo D.J. Prior " Time-lapse misorientation maps for the analysis of electron backscatter diffraction data from evolving microstructures" *Scripta Materialia* 65 (2011) 600
- [23] B.S El-Dasher, B.L Adams, A.D Rollett "Viewpoint: experimental recovery of geometrically necessary dislocation density in polycrystals" *Scripta Materialia* 48 (2003) 141
- [24] D.P. Field, P.B. Trivedi, S.I. Wright, M. Kumar "Analysis of local orientation gradients in deformed single crystals" *Ultramicroscopy* 103 (2005) 33
- [25] W. Pantleon "Resolving the geometrically necessary dislocation content by conventional electron backscattering diffraction" *Scripta Materialia* 58 (2008) 994
- [26] J. Wheeler, E. Mariani, S. Piazzolo, D.J. Prior, P. Trimby, M.R. Drury "The weighted Burgers vector: a new quantity for constraining dislocation densities and types using electron backscatter diffraction on 2D sections through crystalline materials" *Journal Of Microscopy-Oxford*, 233 (2009) 482

